Cooperative Effects and Strengths of Hydrogen Bonds in Open-Chain *cis*-Triaziridine Clusters ($n = 2-8$): A DFT Investigation

Hua-Jie Song,*,†,‡ He-Ming Xiao,† Hai-Shan Dong,‡ and Wei-Hua Zhu†

Department of Chemistry, Nanjing University of Science and Technology, Nanjing 210094, China, and Institute of Chemical Materials, China Academy of Engineering Physics, Mianyang 621900, China

Received: September 22, 2005; In Final Form: December 22, 2005

We employ DFT/B3LYP method to investigate linear open-chain clusters ($n = 2-8$) of the *cis*-triaziridine molecule that is a candidate molecule for high energy density materials (HEDM). Our calculations indicate that the pervasive phenomena of cooperative effects are observed in the clusters of $n = 3-8$, which are reflected in changes in lengths of N···H hydrogen bonds, stretching frequencies, and intensities of N−H bonds, dipole moments, and charge transfers as cluster size increases. The n(N) → σ*(N−H) interactions, i.e., the charge transfers from lone pairs (n(N)) of the N atoms into antibonds (σ*) of the N−H bonds acting as H-donors, can be used to explain the observed cooperative phenomena. The approaches based upon natural bond orbital (NBO) method and theory of atoms in molecule (AIM) to evaluating N···H strengths are found to be equivalent. In the process of N···H bonding, cooperative nature of n(N) → σ*(N−H) interactions promotes formation of stronger N···H bonds as reflected in increases in the capacities of *cis*-triaziridine clusters to concentrate electrons at the bond critical points of N···H bonds. The calculated nonadditive energies also show that the cooperative effects due to n(N) → σ*(N−H) interactions indeed provide additional stabilities for the clusters.

1. Introduction

Hydrazine is an important chemical propellant used for rocket propulsion, and some of its higher derivatives may become promising candidates for high energy density materials (HEDM). These compounds containing the singly bonded >N−N< fragments are destabilized by repulsions between lone pairs.[1] Cyclic triaziridine (viz. cyclotriazane, N_3H_3) must involve two N−N bond breaking for dissociation into two fragments, its activation barrier is expected to be higher than that of its linear analogue. Therefore, it is a potential HEDM molecule. Triaziridine was synthesized first in the form of silver complex[2] early in 1977 and has not been isolated experimentally as a free molecule so far. The triaziridine molecule and its isomers have been extensively studied mainly on the electron energies, thermochemical properties, conformational analyses, and the ring strains of isolated molecules by using ab initio methods.[1,3−10] These studies indicated that the triaziridine system is stable enough to be isolated.

As a candidate for HEDM, the triaziridine system deserves a more extensive theoretical examination. It is becoming clear that nonadditive effects cannot be neglected in quantitative treatments and play key roles in determining many important physical properties.[11] For most H-bonded clusters, the nonadditive energies are negative, and this leads to additional stabilities of the systems that usually exhibit so-called cooperative effects.[12] Our main goal here is to draw main trends in cooperativities of *cis*-triaziridine clusters by employing the B3LYP level of density functional theory (DFT), natural bond orbital (NBO) analysis,[13,14] and Bader's theory of atoms in molecule (AIM).[15,16]

2. Computational Methods

We have computed the optimal geometries and harmonic vibrational frequencies of *cis*-triaziridine clusters up to eight molecules at the B3LYP/6-31++G(d, p) level. The nonadditve energies of the optimized clusters ($n = 3-8$) are also evaluated at the B3LYP/aug-cc-pvdz level using the supermolecule approach (SM),[17] where the counterpoise technique of Boys and Bernardi[18] is used to correct basis set superposition error (BSSE).[19] All the calculations were performed with the Gaussian03 program.[20]

We also try to evaluate strengths of the N···H bonds based upon the NBO method[13,14] and the theory of AIM.[15,16] NBO corresponds closely to the picture of localized bonds and lone pairs as basic units of molecular structure. According to NBO, the shift of electron density as a result of H-bond formation can be identified by comparing the charges of the individual atoms in the uncomplexed and complexed states. Unlike Mulliken or other charge partitioning schemes, NBO scheme is unaffected by the presence of diffuse functions in the basis set adopted here.[14] One has early realized the importance of the role of orbital interactions in H-bonded "van der Waals" molecules.[21] Reed and Weinhold adduced ab initio evidences for the importance of localized n(B) → σ*(A−H) interactions in A−H···B hydrogen bonding,[22] i.e., electronic delocalization from the filled lone pair n(B) of the "Lewis base" B into the unfilled antibond σ*(A−H) of the "Lewis acid" A−H. In the meantime, a number of investigations have employed AIM theory to analyze H-bonds (HBs). Koch and Popelier formulated eight concerted effects occurring in the electron density $\rho(\mathbf{r})$ at the bond critical point (BCP) of HB, which is indicative of hydrogen bonding.[23] Abramov has proposed[24] the evaluation of the local electronic kinetic energy density $G(\mathbf{r})$ in terms of $\rho(\mathbf{r})$, and its gradient $\nabla\rho(\mathbf{r})$, and Laplacian $\nabla^2\rho(\mathbf{r})$ for closed

† Nanjing University of Science and Technology.
‡ China Academy of Engineering Physics.
* Corresponding author. E-mail: hjsongmoru@tom.com.

10.1021/jp055385s CCC: $33.50
Published on Web 01/24/2006

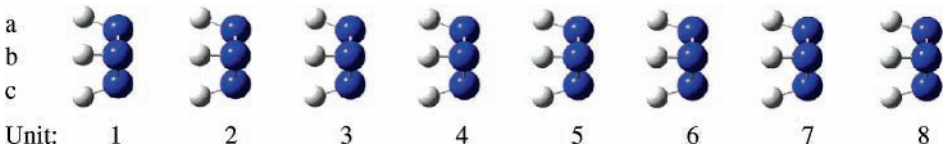

Figure 1. Open chain structure of *cis*-triaziridine octamer. A general rule about labeling atoms in the clusters ($n = 2-8$) is also given. For example, N(2b) means the N of unit 2 lies in chain "b".

TABLE 1: Geometric, Dielectric and Vibrational Properties of *cis*-Triaziridine Clusters ($n = 1-8$) at the B3LYP/6-31++G(d,p) Level

		geometric parameters[a]		dielectric properties[b]		N−H stretching vibration[c]			
		R_{N-N} (nm)	R_{N-H} (nm)	q_{CT} (e)	μ (D)	I_m (km mol^{-1})	ν_m (cm^{-1})	I_s (km mol^{-1})	ν_s (cm^{-1})
isolated molecule		0.146 55	0.102 98		4.11			19.7	3371.9
dimer	unit1	0.146 36	0.102 86	0.026 65	9.50	14	3377.9	9.2	3397.7
	unit2	0.146 79	0.102 96	−0.02665					
trimer	unit1	0.146 29	0.102 82	0.035 15	15.50	79	3371.3	5.3	3405.7
	unit2	0.146 62	0.102 95	0.001 55					
	unit3	0.146 83	0.103 00	−0.03669					
tetramer	unit1	0.146 33	0.102 81	0.038 95	21.82	218	3366.2	2. 9	3409.1
	unit2	0.146 57	0.102 96	0.009 35					
	unit3	0.146 68	0.103 02	−0.00685					
	unit4	0.146 87	0.103 03	−0.04145					
pentamer	unit1	0.146 33	0.102 81	0.040 91	28.30	548	3361.5	1.9	3411.0
	unit2	0.146 55	0.102 96	0.012 40					
	unit3	0.146 64	0.103 05	0.000 97					
	unit4	0.146 70	0.103 07	−0.01085					
	unit5	0.146 89	0.103 04	−0.04343					
hexamer	unit1	0.146 32	0.102 80	0.041 95	34.93	950	3354.4	1.3	3411.7
	unit2	0.146 55	0.102 97	0.014 42					
	unit3	0.146 62	0.103 07	0.004 00					
	unit4	0.146 67	0.103 11	−0.00267					
	unit5	0.146 72	0.103 10	−0.01280					
	unit6	0.146 88	0.103 04	−0.04491					
heptamer	unit1	0.146 32	0.102 80	0.042 16	41.60	1354	3346.9	1.1	3411.8
	unit2	0.146 55	0.102 98	0.015 78					
	unit3	0.146 63	0.103 09	0.006 01					
	unit4	0.146 66	0.103 13	0.000 34					
	unit5	0.146 69	0.103 15	−0.00476					
	unit6	0.146 73	0.103 11	−0.01421					
	unit7	0.146 90	0.103 05	−0.04531					
octamer	unit1	0.146 29	0.102 80	0.042 96	48.36	1796	3341.0	1.1	3412.2
	unit2	0.146 52	0.102 97	0.015 97					
	unit3	0.146 60	0.103 09	0.006 91					
	unit4	0.146 63	0.103 16	0.002 08					
	unit5	0.146 65	0.103 17	−0.00161					
	unit6	0.146 66	0.103 16	−0.00505					
	unit7	0.146 72	0.103 15	−0.01559					
	unit8	0.146 86	0.103 15	−0.04567					

[a] These entities listed here are average lengths of three N−N (or N−H) bonds for each monomer units. [b] These entities are estimated at the B3LYP/aug-cc-pvdz level. [c] *I* is for intensity; ν is for frequency.

shell interactions. Espinosal et al. applied Abramov's proposal to finding out the fact that local electronic potential energy density $V(\mathbf{r}_{cp})$ at the BCP of O···H hydrogen bond doubles the dissociation energy of the HB[25] and to obtaining the dependence of the total electron energy density at the BCP of the O···H against interatomic distance.[26] We also extend the proposal to looking at $\rho(\mathbf{r}_{cp})$, $\nabla^2\rho(\mathbf{r}_{cp})$, $G(\mathbf{r}_{cp})$ and $V(\mathbf{r}_{cp})$ of the N···H bonds of the *cis*-triaziridine clusters. According to AIM theory, $G(\mathbf{r})$ and $V(\mathbf{r})$ conform to the local form of the virial theorem.[15]

3. Results and Discussion

3.1. Geometries. As shown in Figure 1, the optimized geometries for these clusters ($n = 2\sim8$) are of linear open chain structures and two neighbor monomers in them are bound by three N···H bonds. The lengths of N−N and N−H bonds are collected in Table 1 and all of the N···H lengths are listed in Table 2.

The N−N bonds of the clusters ($n = 2-8$) fall into two categories: N−N of unit 1 and N−N of the others (unit 2-*n*) acting as H-donors. Relative to N−N (0.14655 nm) of isolated molecules, N−N bonds of unit 1 are shortened and those of unit 2−*n* are elongated. However, N−N of unit 1 does not exhibit a cooperative change with cluster size. The average N−N lengths of unit 2−*n* are as follows: 0.14679 nm for dimer, 0.14673 nm for trimer, 0.14671 nm for tetramer, 0.14670 nm for pentamer, 0.14669 nm for hexamer, 0.14669 nm for heptamer, and 0.14666 nm for octamer, respectively. The magnitude of the bond elongation decreases slightly.

Since N−H of unit 1 is not a H-donor, its length for each cluster ($n = 2-8$) diminishes compared with N−H (0.10298 nm) of the isolated molecule, but this decrement is quickly saturated. For N−H bonds of other units, their average lengths are 0.10296 nm for dimer, 0.10298 nm for trimer, 0.10300 nm for tetramer, 0.10303 nm for pentamer, 0.10306 nm for hexamer,

TABLE 2: N···H Lengths (nm), NBO Stabilization Energies (kJ/mol), Local Electronic Kinetic Energy Densities (kJ/mol), and Local Electronic Potential Energy Densities (kJ/mol) at N···H BCP

n	N···H[a]	R_N···H	$E_{n(N)\rightarrow\sigma^*(2)}$	G($\mathbf{r}_{cp}$)	V($\mathbf{r}_{cp}$)	*n*	N···H[a]	R_N···H	$E_{n(N)\rightarrow\sigma^*(2)}$	G($\mathbf{r}_{cp}$)	V($\mathbf{r}_{cp}$)
2	1a···2a	0.239 25	−12.247	19.207	−20.490	7	1a···2a	0.226 02	−20.148	26.355	−26.901
	1b···2b	0.238 10	−12.833	19.754	−21.011		1b···2b	0.225 97	−20.189	26.396	−26.936
	1c···2c	0.237 28	−13.209	20.144	−21.375		1c···2c	0.226 35	−19.897	26.146	−26.740
3	1a···2a	0.229 98	−17.263	23.987	−24.945		2a···3a	0.218 57	−26.877	32.217	−31.531
	1b···2b	0.230 28	−17.054	23.805	−24.795		2b···3b	0.218 60	−26.836	32.187	−31.510
	1c···2c	0.230 45	−16.929	23.680	−24.688		2c···3c	0.218 82	−26.627	31.995	−31.369
	2a···3a	0.230 68	−17.305	23.714	−24.691		3a···4a	0.216 40	−29.302	34.211	−33.099
	2b···3b	0.232 56	−16.009	22.538	−23.664		3b···4b	0.216 42	−29.302	34.188	−33.082
	2c···3c	0.232 00	−16.344	22.855	−23.940		3c···4c	0.216 58	−29.135	34.046	−32.981
4	1a···2a	0.227 39	−18.977	25.520	−26.230		4a···5a	0.216 56	−29.260	34.091	−33.049
	1b···2b	0.227 61	−18.852	25.375	−26.112		4b···5b	0.216 68	−29.218	34.080	−33.041
	1c···2c	0.227 87	−18.685	25.229	−25.999		4c···5c	0.216 57	−29.135	33.988	−32.975
	2a···3a	0.223 70	−22.154	28.188	−28.467		5a···6a	0.218 83	−26.919	32.119	−31.609
	2b···3b	0.222 95	−22.823	28.785	−28.928		5b···6b	0.218 83	−26.919	32.120	−31.610
	2c···3c	0.223 78	−22.112	28.158	−28.452		5c···6c	0.218 89	−26.836	32.064	−31.569
	3a···4a	0.227 74	−19.437	25.558	−26.324		6a···7a	0.227 97	−19.479	25.261	−26.131
	3b···4b	0.229 95	−17.765	24.038	−25.050		6b···7b	0.228 00	−19.437	25.251	−26.126
	3c···4c	0.230 02	−17.723	23.988	−25.003		6c···7c	0.228 06	−19.437	25.221	−26.103
5	1a···2a	0.226 13	−19.897	26.317	−26.873	8	1a···2a	0.225 57	−20.440	26.652	−27.141
	1b···2b	0.226 27	−19.771	26.218	−26.794		1b···2b	0.225 62	−20.440	26.623	−27.119
	1c···2c	0.226 82	−19.479	25.903	−26.558		1c···2c	0.225 61	−20.440	26.634	−27.130
	2a···3a	0.220 34	−25.247	30.817	−30.484		2a···3a	0.218 31	−27.170	32.423	−31.682
	2b···3b	0.219 48	−26.041	31.542	−31.012		2b···3b	0.218 29	−27.212	32.442	−31.696
	2c···3c	0.223 48	−22.321	28.193	−28.488		2c···3c	0.218 26	−27.212	32.468	−31.717
	3a···4a	0.220 85	−24.787	30.370	−30.225		3a···4a	0.215 67	−30.096	34.885	−33.585
	3b···4b	0.220 29	−25.331	30.857	−30.593		3b···4b	0.215 62	−30.180	34.928	−33.616
	3c···4c	0.222 03	−23.910	29.563	−29.640		3c···4c	0.215 64	−30.138	34.907	−33.603
	4a···5a	0.228 43	−19.103	25.056	−25.946		4a···5a	0.215 05	−30.890	35.506	−34.076
	4b···5b	0.228 50	−18.935	24.944	−25.841		4b···5b	0.214 97	−30.974	35.585	−34.134
	4c···5c	0.228 93	−18.601	24.637	−25.579		4c···5c	0.215 01	−30.932	35.543	−34.106
6	1a···2a	0.225 74	−20.231	26.576	−27.084		5a···6a	0.215 95	−30.012	34.659	−33.473
	1b···2b	0.225 78	−20.231	26.557	−27.073		5b···6b	0.215 91	−30.054	34.692	−33.497
	1c···2c	0.226 09	−19.980	26.338	−26.899		5c···6c	0.215 95	−30.012	34.658	−33.475
	2a···3a	0.219 23	−26.209	31.666	−31.123		6a···7a	0.217 91	−27.797	32.917	−32.201
	2b···3b	0.219 24	−26.209	31.664	−31.125		6b···7b	0.217 88	−27.797	32.941	−32.219
	2c···3c	0.219 67	−25.791	31.283	−30.843		6c···7c	0.217 94	−27.755	32.890	−32.184
	3a···4a	0.218 21	−27.504	32.587	−31.899		7a···8a	0.227 55	−19.730	25.594	−26.433
	3b···4b	0.218 24	−27.463	32.559	−31.879		7b···8b	0.227 50	−19.771	25.633	−26.466
	3c···4c	0.218 29	−27.421	32.514	−31.843		7c···8c	0.227 70	−19.604	25.497	−26.356
	4a···5a	0.219 60	−26.083	31.445	−31.085						
	4b···5b	0.219 51	−26.167	31.538	−31.154						
	4c···5c	0.219 49	−26.209	31.554	−31.166						
	5a···6a	0.227 91	−19.395	25.319	−26.174						
	5b···6b	0.227 68	−19.604	25.484	−26.312						
	5c···6c	0.227 82	−19.479	25.387	−26.233						

[a] In this column, the N and H are labeled in terms of Figure 1.

0.10309 nm for heptamer, and 0.10312 nm for octamer. Clearly, the N−H bonds acting as H-donors become slightly longer as cluster size increases.

Since cooperative changes in N−N and N−H seem not to be marked, it is of interest to note the N···H lengths. This is also because the HB lengths reflect the HB strengths in the geometric sense. It can be seen from Table 2 that in contrast to N−N and N−H there is a conspicuous change in N···H length $R_{N\cdots H}$ that is dependent upon chain length. The average values of $R_{N\cdots H}$ for the clusters (n = 3−8) are 0.007 (3.1%), 0.011 (5.0%), 0.014 (6.2%), 0.016 (7.2%), 0.017 (7.9%), and 0.019 nm (8.5%) shorter than the average (0.2382 nm) of the dimer, respectively. A significant N···H shrinkage is already evident in the trimer (about 0.007 nm). What is more, the contraction in the octamer is more than twice this value, reflecting the strongly cooperative effect in the clusters ($n > 2$) and its progressive enhancement with chain length. Since the N−H lengths are almost invariant to chain length of cluster, the remarkable contraction of $R_{N\cdots H}$ in the clusters (n = 3−8) should result in the fact that the total chain length is more than shorter than expected from a noncooperative model based on the dimer geometry. Therefore, the n-dependent variation in N···H length should serve as a useful signature of H bond cooperativity of the *cis*-triaziridine cluster. It can be also found that the N···H shrinkage at size n = 8 seems not to arrive at saturation.

3.2. Stretching Frequencies of N−H. Among the three types of stretching vibrations of N−N, N−H and N···H bonds, the displacements of N−N stretching frequencies are rather weak, and the N···H stretching frequencies are very low and their intensities are weak. Displacement of hydride stretching frequencies has long been recognized as general experimental characteristic of H-bonded systems. So here we will only discuss the normal modes involved in N−H stretching vibrations.

Out of the stretching modes of N−H, two normal modes are regarded as the most important for investigating the cooperativity. One mode designated by "s" is composed of three N−H vibrations on the monomer unit 1, as shown in Figure 2a. The other mode denoted by "m" is synthesized by N−H vibrations on the units other than unit 1, which is shown in Figure 2b. The frequencies of the two modes are listed in Table 1.

As compared with the "s" mode of isolated molecule at 3371.9 cm^{-1}, frequencies of the "s" modes are blueshifted, but

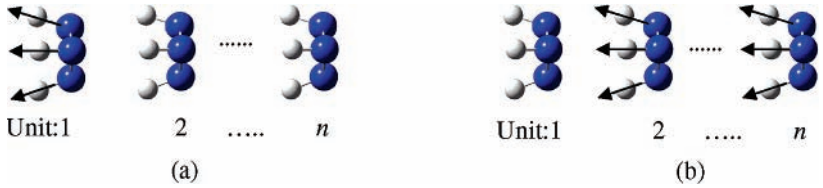

Figure 2. Two important normal modes of N−H stretching vibrations at size *n*. (a) "s" normal mode; (b) "m" normal mode.

increase in the shift with cluster size is small. This is consistent with the slight shortening of N−H of unit 1. IR intensities of the modes are found to diminish with increasing cluster chain. In fact, each "s" mode always corresponds to the maximal frequency of each IR spectrum. On the other hand, frequency of "m" mode takes on an obvious progressive redshift from dimer to octamer. The redshift of octamer is up to 36.9 cm^{-1} relative to dimer. The "m" modes are always at lower frequencies than the "s" modes. Furthermore, we can observe that frequency difference between the two modes, $\Delta_f = \nu_s - \nu_m$ (ν for frequency), enhances with cluster size. Δ_f values for $n = 2-8$ are 19.8, 34.4, 42.9, 49.5, 57.3, 64.9, and 71.2 cm^{-1}, respectively. The evident redshifts of "m" modes and the marked increases in Δ_f with cluster size are signatures of H-bond cooperativities of the *cis*-triaziridine cluster systems.

It can also be observed that the "m" mode is sharply intensified from 14 km/mol for dimer to 1796 km/mol for octamer. As shown in Figure 2b, the stretching mode is synthesized by the N−H stretching vibrations of the "H-donor" monomer units (unit 2−*n*) with a synchronized change in dipole moments of the units, so that the synchronization leads to a maximal variation in total dipole moment of entire cluster during the stretching vibrations and the mode is of maximal IR intensity. More importantly, the strongly nonlinear increase in intensities implies that the dipole difference with respect to the same displacement dramatically enhances with chain length in a cooperative manner. Thereby, it is believed that the nonlinear intensification in the intensities reflects the cooperative nature in the clusters. It has also been recognized that the intensity of A−H stretching mode in A−H···B H-bonded system could be attributed to charge-transfer term in the wave function.[49] For this reason, to consider the dipole moments and charge transfers in the clusters helps understand further the cooperative nature.

3.3. Dipole Moments. The dipole moments (μ) are calculated at the B3LYP/Aug-cc-pvdz level. The average dipole moments per monomer unit for the clusters ($n = 2\sim8$) are 4.75, 5.17, 5.46, 5.66, 5.82, 5.94, and 6.05 D, respectively, and beyond 4.11 D of the isolated molecule by 15.6%, 25.8%, 32.8%, 37.7%, 41.6%, 44.5%, and 47.2% for $n = 2\sim8$, respectively. The marked enhancement with cluster size suggests that *cis*-triaziridine cluster exhibits an increased dipole moment relative to the vector addition of the dipole moments for the monomers. For instance, the dipole moment of the octamer is 15.48 D greater than that expected from a simple additive dipole model. The dipole moment increment of ∼2% from heptamer to octamer illustrates that the incomplete saturation of dielectric cooperativities should be still evident even in the higher clusters ($n > 8$). These additional dipole moments are none other than induced dipole moments arising from inductive phenomena.

3.4. Charge Transfers. The shift in electron density is drawn not only from the lone pair of hydrogen-acceptor atom on a molecule participating in the N···H bond but also from entire molecule. In this work, we first considered the total effect of charge transfer (CT) between monomer units. The net charges q_{CT} of all monomer units originating from the whole CT are derived in terms of NBO analyses of B3LYP/aug-cc-pvdz wave functions. q_{CT} values of the left terminal units (viz, unit 1) for $n = 3-8$ increase relative to that of the dimer by 31.9%, 46.2%, 53.5%, 57.4%, 58.2%, and 61.2%, respectively. The difference enlarges progressively with chain length of cluster. In this sense, the CT interaction is responsible for the "cooperativity dipole" that systematically increases with chain length. Evidently, the cooperativity dipole or the dielectric cooperativity cannot be reduced into pair-additivity such as the ordinary vector sum of monomer dipoles.

Although in principle the shift in density rather than being localized over a particular region delocalizes throughout the acceptor and donor molecules, for a H-bonded system the CT arising from HB contributions should be taken especially into consideration. Thereby, the actual magnitudes of the charges transferred from lone pairs (n(N)) of the hydrogen bonded N atoms on one units into antibonds (σ^*) of the N−H bonds on other units being H-donors, i.e., the real quantities $q_{n(N)\rightarrow\sigma^*}$ of charge transfers due to the n(N) → σ^*(N−H) interactions, are evaluated according to reference 14. In terms of the derived $q_{n(N)\rightarrow\sigma^*}$, we also calculate the net charges (q_{CT-HB}) distributed over monomers as result of the n(N) → σ^*(N−H) and compared them with q_{CT}. A linear relation of a good correlation factor ($r = 0.998$) between q_{CT-HB} and q_{CT} can be expressed by

$$q_{CT-HB} = 0.58\, q_{CT} \qquad (1)$$

In this way, q_{CT-HB} reflecting distribution of the net charges due to n(N) → σ^* interactions over the H-bonded monomers accounts for more than 50% of q_{CT} as result of the whole CT that delocalizes entirely the two molecule units bound by three H-bonds. N···H bonding contributes substantially to the subtle shifts in the electron densities of the cluster molecules. Expressed another way, three N···H bonds linking two monomers play important roles in the total CT interactions between the two monomer molecules.

Furthermore, it can be observed that q_{CT} are distributed in the nonequilibrium way that the strongest net charges are at the two terminal units and then attenuate rapidly toward the interior units. Because of the linear relationship between q_{CT-HB} and q_{CT}, there is reason to believe that a similar nonequilibrium way of charge distribution along HB chain should be also existent. On no account does this mean that the CT interactions between interior units are much weaker than those at the two ends. This is because the interior monomer unit of the general $(HN)_3\cdots(HN)_3\cdots$ chain accepts a smaller quantity of charge than it donates if the chain extends farther on left terminal unit (electron donor side), and the case is contrary if it extends toward the acceptor side. Both q_{CT} and q_{CT-HB} for the interior units describe only the net charges and hence are not used to describe the actual magnitude of CT that should be reflected by $q_{n(N)\rightarrow\sigma^*}$ to a certain extent. As a matter of fact, for each clusters ($n > 2$) the most powerful CT always arises between the two intermediate units, which can be illustrated by Figure 3. In this way, we believe that the n(N) → σ^* interactions are likely to contribute rather importantly to the nonlinear cooperative effects of pronounced *n*-dependency.

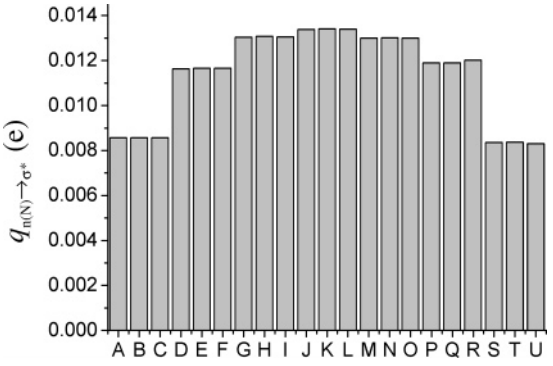

Figure 3. $q_{n(N)\to\sigma^*}$ of *cis*-triaziridine octamer. A, B, C, ..., T, and U denote N(1a)···H(2a), N(1b)···H(2b), N(1c)···H(2c), ..., N(7b)···H(8b), and N(7c)···H(8c), respectively.

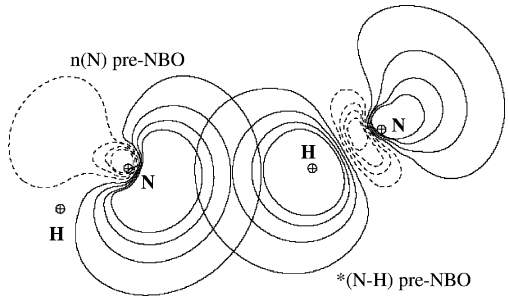

Figure 4. Contour plots of the overlap of pre-NBOs of lone pair n(B) of unit 1 with antibonding orbital σ^* (N−H) of unit 2 associated with intermolecular N···N−H hydrogen bond formation for *cis*-triaziridine dimer. Atomic positions are indicated by circled crosses. The outermost contours are at 0.03 au, and the contour interval is 0.05 au.

3.5. Strengths of N···H Hydrogen Bonds. It may be expected that H-bond energy can directly and explicitly characterize interaction between hydrogen-bonded atoms. Unfortunately, a clear quantum mechanics (QM) definition on it has not been given up to now and there is no single way to obtain a reliable estimate of the H-bond energy.

As illustrated in Figure 4, the orbital overlap between n(N) and σ^*(N−H) is associated with the formation of intermolecular N···H. The overlap and the corresponding CT lead to energetic stabilization of the H-bonded systems. The stabilization energy ($E_{n(N)\to\sigma^*}^{(2)}$)[14] due to the n(N)→$\sigma^*$(N−H) interaction can reflect attractive interaction in N···H bonding. So it offers us a theoretical approach to characterizing H-bond strengths in this work. We derive$E_{n(N)\to\sigma^*}^{(2)}$ of each H-bond according to ref 14. A correlation between $\ln(-E_{n(N)\to\sigma^*}^{(2)})$ and $R_{N\cdots H}$ for the 84 H-bonds of the equilibrium geometries is found as follows:

$$\ln(-E_{n(N)\to\sigma^*}^{(2)}) = 11.55 - 37.77R_{N\cdots H} \qquad (2)$$

This correlation of $r = 0.998$ lends the credence to the argument mentioned previously, i.e., the n(N)→ σ^*(N−H) interaction contributes importantly to the cooperative nature that leads to the conspicuous contraction in N···H. Among the 84 HBs, the weakest HB ($E_{n(N)\to\sigma^*}^{(2)} = -12.2$ kJ/mol) is the N(1a)···H(2a) of dimer and its $R_{N\cdots H}$ is a maximum of 0.2392 nm. In contrast, the N(4b)···H(5b) at $n = 8$ is the strongest H-bond ($E_{n(N)\to\sigma^*}^{(2)} = -31.0$ kJ/mol) and has the largest N···H contraction of up to −0.0242 nm. The average values of $E_{n(N)\to\sigma^*}^{(2)}$ per monomer from $n = 2$ to 8 are 12.76, 16.8, 19.8, 22.0, 23.9, 25.3, and 26.6 kJ/mol, respectively. Very clearly, the increased average shows that the HB strength enhances with cluster size. However, we also note that this increment from n to $n + 1$ decays gradually with cluster size (n) enlarging. For example, the increment from dimer to trimer is 4.0 kJ/mol, the increment from heptamer to octamer decreases up to 1.3 kJ/mol. However, the increment of 1.3 kJ/mol reminds us that there is a certain margin for enhancement of H-bond strength and contraction of H-bond length in the higher cluster ($n > 8$). It is also observed that the distribution of $E_{n(N)\to\sigma^*}^{(2)}$ is similar to that of $q_{n(N)\to\sigma^*}$, that is, the strongest HB of each clusters lies between two intermediate units.

On the other hand, hydrogen bond can be characterized by an area of low electronic density and by the appearance of a critical point in the gradient of the density. Therefore, AIM theory provides us an alternative approach to exploring nature of intermolecular hydrogen bonding by studying electron densities in vicinity of the N···H hydrogen bonds of the equilibrium geometries. The topological analyses of the B3LYP/aug-cc-pvdz electron densities of the clusters have been performed using the AIM2000 program.[27] Thus, we derive electron densities $\rho(\mathbf{r}_{cp})$ and their Laplacian $\nabla^2\rho(\mathbf{r}_{cp})$ of the 84 H-bonds. The positive $\nabla^2\rho(\mathbf{r}_{cp})$ is of the same order of magnitude as $\rho(\mathbf{r}_{cp})$ ($\sim 10^{-2}$ au). They have the general characteristic of the H-bond that has been pointed out by many studies,[28] and they have the following respective dependencies upon $R_{N\cdots H}$: $\ln \rho(\mathbf{r}_{cp}) = 0.62 - 20.99R_{N\cdots H}$, $r = 0.999$; $\ln\nabla^2\rho(\mathbf{r}_{cp}) = 1.83 - 22.05R_{N\cdots H}$, $r = 0.999$. The energetic parameters ($G(\mathbf{r}_{cp})$ and $V(\mathbf{r}_{cp})$) for the HB can be further obtained from the Abramov expression[25] and the local form of the virial theorem.[15] The two energetic parameters are listed in Table 2. $\ln G(\mathbf{r}_{cp})$ against $R_{N\cdots H}$ is linear ($\ln G(\mathbf{r}_{cp}) = 9.13 - 25.89 R_{N\cdots H}$, $r = 0.999$). Similarly, $V(\mathbf{r}_{cp})$ follows an exponential dependence on $R_{N\cdots H}$ ($\ln(-V(\mathbf{r}_{cp})) = 10.04 - 30.17R_{N\cdots H}$, $r = 0.999$), although with a slightly different exponential factor.

The similar dependencies of $V(\mathbf{r}_{cp})$, $G(\mathbf{r}_{cp})$, and $E_{n(N)\to\sigma}{}^{*(2)}$ upon $R_{N\cdots H}$ uncover the correlation of $V(\mathbf{r}_{cp})$ and $G(\mathbf{r}_{cp})$ with $E_{n(N)\to\sigma^*}^{(2)}$, The relationships assume good linear correlations of $r > 0.999$:

$$V(\mathbf{r}_{cp}) = -5.271 - 0.965E_{n(N)\to\sigma^*}{}^{(2)} \qquad (3)$$

and

$$G(\mathbf{r}_{cp}) = 8.706 + 0.872E_{n(N)\to\sigma^*}{}^{(2)} \qquad (4)$$

From these, we believe that as cluster size increases, the magnitude of $E_{n(N)\to\sigma^*}^{(2)}$ heightens as result of cooperatively enhanced n(N)→σ^*(N−H) interaction, and hence leads to N···H contractions in a nonlinear way and formation of stronger HB as also reflected in increase in $\rho(\mathbf{r}_{cp})$. In terms of AIM theory, $V(\mathbf{r}_{cp})$ represents the capacity of *cis*-triaziridine cluster to concentrate electrons at BCP of the N···H bond. Therefore, the increased $\rho(\mathbf{r}_{cp})$ is translated into a higher potential energy $V(\mathbf{r}_{cp})$. On the other hand, however, more repulsion that has to be triggered to resist this contraction for avoiding infringement of the Pauli principle enhances the ability of the system to dilute the accumulated electrons at the BCP, and thus heightening $G(\mathbf{r}_{cp})$, which gives the tendency of the cluster to dilute electrons at the BCP. Therefore, in this sense, the enhanced $G(\mathbf{r}_{cp})$ reflects the accumulation of electron density. Clearly, in the case of equilibrium clusters, $V(\mathbf{r}_{cp})$ and $G(\mathbf{r}_{cp})$ reflect, from two different points of view, the same physical process, i.e., how the electrons around the critical point are affected by the HB interaction. According to the description of N···H bonding, $E_{n(N)\to\sigma^*}^{(2)}$ and $V(\mathbf{r}_{cp})$ (or $G(\mathbf{r}_{cp})$) are identical quantities for characterizing HB strengths, i.e., the NBO and AIM strengths are equivalent. In this way, we believe that the cooperative nature of n(N) →

TABLE 3: Binding Energies, Nonadditive Energies, and Zero Point Energies for the *cis*-Triazidine Clusters (in kJ·mol^{-1})

	E_{ZPE}	E_b	E_{NA}	E_{NA} vs E_b (%)
isolated molecule	119.98			
dimer	246.11	−22.17		
trimer	373.99	−55.41	−9.36	16.9
tetramer	502.58	−94.53	−24.98	26.4
pentamer	630.80	−137.66	−44.40	32.3
hexamer	759.90	−182.09	−66.67	36.6
heptamer	888.71	−228.13	−90.49	39.7
octamer	1017.53	−274.78	−115.86	42.2

σ^*(N−H) should be responsible for enhancement in strengths of N···H in the clusters.

3.6. Nonadditive Energies. Nonadditive energy is calculated as the difference between the combined interaction energy of molecular pairs and the interaction energy of the complex. The nonadditive energies (E_{NA}) of these clusters at the B3LYP/aug-cc-pvdz levels are collected in Table 3. The binding energies (E_b) of the clusters which account for zero point energy corrections are also listed in the Table 3.

It can be seen from the Table 3 that E_{NA} are negative and increase with cluster size. This fact indicates that the cooperative effects due to n(N) → σ^*(N−H) interactions indeed provide additional stabilities for the systems that exhibit cooperative changes in relevant properties previously mentioned. Although the conspicuous N···H contraction causes instability of system, cooperative nature of the n(N) → σ^*(N−H) interactions plays a key role in overcoming the instability and further stabilizing the system. In addition, E_{NA} vs E_b from heptamer to octamer increases by up to 2.5%. This illustrates once more that at size $n = 8$ the cooperative effect is not saturated yet.

Summary and Conclusions

We have employed DFT/B3LYP, NBO and AIM to investigate structural, dielectric and vibrational properties of the *cis*-triazidine clusters up to eight molecules and their strengths of N···H H-bonds as well as nonadditive interaction energies. Our results indicate that cooperative phenomenon is pervasive in the clusters, as reflected in changes in N···H lengths, N−H stretching frequencies and intensities, dipole moments, and charge transfers with increasing cluster size (n).

According to NBO, the cooperative change can be explained by intermolecular n(N) → σ^*(N−H) interaction between H-bonded atoms. Since the stabilization energy ($E_{n(N)\rightarrow\sigma^*}^{(2)}$) as a result of n(N) → σ^*(N−H) is able to reflect attractive interaction in hydrogen bonding and hence can be used to characterize the strength of N···H H-bond in this work. In particular, good linear correlations of $E_{n(N)\rightarrow\sigma^*}^{(2)}$ with the local kinetic potential energies ($G(\mathbf{r}_{cp})$) and local potential energies ($V(\mathbf{r}_{cp})$) at bond critical points of N···H bonds are found. Hence, we believe that the magnitude of $E_{n(N)\rightarrow\sigma^*}^{(2)}$ heightens as clusters size increases, which provides a driving force for N···H contraction in a nonlinear way and promotes formation of stronger N···H as reflected in the increase in electron density at BCP of the N···H. The increased density is translated into a higher potential energy $V(\mathbf{r}_{cp})$. At the same time, stronger repulsion counteracting this contraction enhances the ability of system in diluting this accumulated electrons at the BCP, and therefore heightening $G(\mathbf{r}_{cp})$ that gives the tendency of the cluster to dilute electrons at the BCP. In this way, $V(\mathbf{r}_{cp})$ and $G(\mathbf{r}_{cp})$ can be used to characterize HB strengths in the equilibrium clusters as well and the HB strengths are equivalent to those represented by $E_{n(N)\rightarrow\sigma^*}^{(2)}$

The calculated nonadditive energies are negative and increase with cluster size, This indicates that the cooperative effects due to the n(N) → σ^*(N−H) interactions indeed provide additional stabilities for the systems that exhibit cooperative changes in properties. In addition, from energetic viewpoint, the cooperativity at cluster size of $n = 8$ is still of an incomplete saturation, as also found in the trend of changes in dielectric properties, N···H lengths, and HB strengths.

Acknowledgment. This work is Research Project 42101030410 of Institute of Chemical Materials and was supported partially by the National Natural Science Foundation of China (Grant No. 20173028).

Supporting Information Available: Tables giving computational data about $\rho(\mathbf{r}_{cp})$, $\nabla^2\rho(\mathbf{r}_{cp})$, and $q_{n(N)\rightarrow\sigma^*}$ and Cartesian coordinates of optimized geometries as well as text giving the complete ref 20. This material is available free of charge via the Internet at http://pubs.acs.org.

References and Notes

(1) Schlegel, H. B.; Skancke, A. *J. Am. Chem. Soc.* **1993**, *115*, 7465−7411.
(2) Kim, Y.; Seff, K. *J. Am. Chem. Soc.* **1977**, *99*, 7057−7059.
(3) Nguyen, M. T.; Kaneti, J.; Hoesch, L.; Dreiding, A. S. *Helv. Chim. Acta* **1984**, *67*, 1918−1929.
(4) Magers, D. H.; Salter, E. A.; Bartlett, R. J.; Salter, C.; Hess, B. H., Jr.; Schaadll, L. J. *J. Am. Chem. Soc.* **1988**, *110*, 3435−3446.
(5) Salter, E. A.; Hinrichs, R. Z.; Salter, C. *J. Am. Chem. Soc.* **1996**, *118*, 227−228.
(6) Inagaki, S.; Ishitani, Y.; Kakefu, T. *J. Am. Chem. Soc.* **1994**, *116*, 5954−5958.
(7) Zhao, M.; Gimarc, B. M. *J. Phys. Chem.*, **1994**, *98*, 7497−7503.
(8) Alcamí, M.; Mó, O.; Yáñez, M. *J. Mol. Struct. (THEOCHEM)* **1998**, *433*, 217−225.
(9) Glukhovtsev, M. N.; Bach, R. D.; Laiter, S. *Int. J. Quantum Chem.* **1997**, *62*, 373−384.
(10) Alcamí, M.; Mó, O.; Yáñez, M.; Alkorta, I.; Elguero, J. *Phys. Chem. Chem. Phys.* **2002**, *4*, 2123−2129.
(11) Elrod, M. J.; Saykally, R. J. *Chem. Rev.* **1994**, *94*, 1975−1997.
(12) Shimizu, S.; Chan, H. S. *J. Chem. Phys.* **2001**, *115*, 3424−3431.
(13) Weinhold, F. *NBO5.0 Program Mnaual*; Theoretical Chemistry Institute: University of Wisconsin, Madison, WI, 2001.
(14) Reed, A. E.; Curtiss, L. A.; Weinhold, F. *Chem. Rev.* **1988**, *88*, 899−926.
(15) Bader, R. F. W. *Acc. Chem. Res.* **1985**, *18*, 9−15.
(16) Bader, R. F. W. *Atoms in Molecules: a Quantumn Theory*. The International Series of Monomgraphs in Chemistry. Clarendon Press: Oxford, 1990.
(17) Chałasinski, G.; Szczesniak, M. M. *Chem. Rev.* **2000**, *100*, 4227−4252.
(18) Boys, S. F.; Bernardi, F. *Mol. Phys.* **1970**, *19*, 553−559.
(19) van Duijneveldt, F. B.; van Duijneveldt-van de Rijdt, J. G. C. M.; van Lenthe, J. H. *Chem. Rev.* **1994**, *94*, 1873−1885.
(20) Frisch, M. J.; et al. Gaussian 03, Revision B.05. Gaussian, Inc.: Pittsburgh, PA, 2003.
(21) Baiocchi, F. A.; Reiher, W.; Klemperer, W. *J. Chem. Phys.* **1983**, *79*, 6428−6429.
(22) Weinhold, F. *J. Mol. Struct. (THEOCHEM)* **1997**, *398*−*399*, 181−197.
(23) Koch, U.; Popelier, P. L. A. *J. Phys. Chem.* **1995**, *99*, 9747−9754.
(24) Abramov, Yu. A. *Acta Crystallogr.* **1997**, *A53*, 264−272.
(25) Espinosa, E.; Molins, E.; Lecomte, C. *Chem. Phys. Lett.* **1998**, *285*, 170−173.
(26) Espinosa, E.; Molins, E. *J. Chem. Phys.* **2000**, *113*, 5686−5694.
(27) AIM2000 homepage: http://www.aim2000.de.
(28) Bone, R. G. A.; Bader, R. R W. *J. Phys. Chem.* **1996**, *100*, 10892−10911 and references therein.